ORNL/TM-2014/513

# STATUS OF HIGH FLUX ISOTOPE REACTOR IRRADIATION OF SILICON CARBIDE/SILICON CARBIDE JOINTS


Approved for public release;
distribution is unlimited.


Yutai Katoh
Takaaki Koyanagi
Jim Kiggans
Nesrin Cetiner
Joel McDuffee


**September 2014**


OAK RIDGE NATIONAL LABORATORY
MANAGED BY UT-BATTELLE FOR THE US DEPARTMENT OF ENERGY

## DOCUMENT AVAILABILITY

Reports produced after January 1, 1996, are generally available free via US Department of Energy (DOE) SciTech Connect.

***Website*** http://www.osti.gov/scitech/

Reports produced before January 1, 1996, may be purchased by members of the public from the following source:

National Technical Information Service
5285 Port Royal Road
Springfield, VA 22161
***Telephone*** 703-605-6000 (1-800-553-6847)
***TDD*** 703-487-4639
***Fax*** 703-605-6900
***E-mail*** info@ntis.gov
***Website*** http://www.ntis.gov/help/ordermethods.aspx

Reports are available to DOE employees, DOE contractors, Energy Technology Data Exchange representatives, and International Nuclear Information System representatives from the following source:

Office of Scientific and Technical Information
PO Box 62
Oak Ridge, TN 37831
***Telephone*** 865-576-8401
***Fax*** 865-576-5728
***E-mail*** reports@osti.gov
***Website*** http://www.osti.gov/contact.html

**ORNL/TM-2014/513**

Materials Science and Technology Division
Reactors and Nuclear Systems Division

# STATUS OF HIGH FLUX ISOTOPE REACTOR IRRADIATION OF SILICON CARBIDE/SILICON CARBIDE JOINTS

Yutai Katoh
Takaaki Koyanagi
Jim Kiggans
Nesrin Cetiner
Joel McDuffee

September 2014:

Prepared by
OAK RIDGE NATIONAL LABORATORY
Oak Ridge, Tennessee 37831-6283
managed by
UT-BATTELLE, LLC
for the
US DEPARTMENT OF ENERGY
under contract DE-AC05-00OR22725

# CONTENTS

**Page**

**LIST OF FIGURES**

**Figure** **Page**

## LIST OF TABLES

**Table** **Page**

## ACKNOWLEDGEMENT

This work was sponsored by the U.S. Department of Energy, Office of Nuclear Energy, for the Light Water Reactor Sustainability (LWRS) program under contact DE-AC05-00OR22725 with Oak Ridge National Laboratories managed by UT-Battelle, LLC. Irradiation in the High Flux Isotope Reactor is sponsored by the Scientific User Facilities Division, Office of Basic Energy Sciences, U.S. Department of Energy.

## EXECUTIVE SUMMARY

Development of silicon carbide (SiC) joints that retain adequate structural and functional properties in the anticipated service conditions is a critical milestone toward establishment of advanced SiC composite technology for the accident-tolerant light water reactor (LWR) fuels and core structures. Neutron irradiation is among the most critical factors that define the harsh service condition of LWR fuel during the normal operation. The overarching goal of the present joining and irradiation studies is to establish technologies for joining SiC-based materials for use as the LWR fuel cladding. The purpose of this work is to fabricate SiC joint specimens, characterize those joints in an unirradiated condition, and prepare rabbit capsules for neutron irradiation study on the fabricated specimens in the High Flux Isotope Reactor (HFIR). Torsional shear test specimens of chemically vapor-deposited SiC were prepared by seven different joining methods either at Oak Ridge National Laboratory or by industrial partners. The joint test specimens were characterized for shear strength and microstructures in an unirradiated condition. Rabbit irradiation capsules were designed and fabricated for neutron irradiation of these joint specimens at an LWR-relevant temperature. These rabbit capsules, already started irradiation in HFIR, are scheduled to complete irradiation to an LWR-relevant dose level in early 2015.

# 1. INTRODUCTION

Development of silicon carbide (SiC) joints that retain adequate mechanical and functional properties in the anticipated service conditions is a critical milestone toward establishment of advanced SiC composite technology for the light water reactor (LWR) fuels and core structures [1, 2]. Neutron irradiation is among the most critical factors that define the service condition of LWR fuel during the normal operation. For the purpose of determining the effects on neutron irradiation at an LWR-relevant temperature on strength and microstructures of the candidate SiC joints, torsional shear test specimens were fabricated using chemically vapor-deposited (CVD) SiC as the substrate material at Oak Ridge National Laboratory or by industrial partners, evaluated for shear strength and microstructures in an unirradiated condition, and prepared for neutron irradiation in the High Flux Isotope Reactor (HFIR) [3]. This report provides detailed information of the joint materials prepared, the method of strength evaluation, and the test matrix for neutron irradiation.

# 2. MATERIALS

## 2.1 MATERIALS PREPARED FOR IRRADIATION STUDY

For the present irradiation experiment, the various SiC joints were prepared using diffusion bonding with the active titanium and molybdenum inserts, transient eutectic-phase (TEP) joining using slurry and green tape, reaction-formed Ti-Si-C MAX-phase bonding, Al-Si-C-O braze-based joining, and hybrid preceramic polymer/chemical vapor infiltration (CVI) joining, as summarized in Table 1.

**Table 1. Silicon carbide – silicon carbide joints prepared for irradiation study**

| Method of joining | Alias | Main phases present in joint layer |
|---|---|---|
| Ti diffusion bonding | Ti dif | Ti3SiC2, TiCx |
| Mo diffusion bonding | Mo dif | Mo4.8Si3C0.6, Mo2C |
| TEP joining using slurry | TEPs | SiC, Y-Al oxides |
| TEP joining using green tape | TEPt | SiC, Y-Al oxides |
| Ti-Si-C MAX-phase bonding | MAX | SiC, Ti3SiC2 |
| Al-Si-C-O braze-based joining | Braze | Al-C-O, Al-Si-C-O and Al-O phases |
| Hybrid preceramic polymer/CVI joining | Polymer/CVI | SiC |

## 2.2 PROCESSING AND MICROSTRUCTURES

The substrates of all the joints were high-purity chemically vapor-deposited (CVD) SiC. Metallographic examinations consisting of combined use of scanning electron microscopy (SEM, S4800, Hitachi) and X-ray diffraction (XRD, Model Scinatag Pad V, Thermo ARL) were performed for characterization of the SiC joints.

### 2.2.1 Titanium diffusion bonding

Pure titanium foil (25 μm thick, 99.94% pure, Alfa-Aesar, Ward Hill, MA) was used for diffusion bonding. The Ti foil joints were fabricated at ORNL. The joining of SiC/metal/SiC sandwiches was accomplished by hot-pressing at 1500 °C, for 1 h, in vacuum, under a uniaxial pressure of 17 MPa.

Estimated partial pressure of oxygen impurity in the furnace was ~0.6 Pa. To reduce oxygen partial pressure in the furnace, titanium powder was used as the oxygen getter. Reduction of oxidation during joining is a key for Ti foil joining to increase the joint strength and to reduce the processing defect at the joint layer, according to our previous work [4].

Cross-sectional backscattered electron image of the Ti foil joint was shown in Figure 1. The joint thickness was ~40 µm. The joint layer exhibited $Ti_3SiC_2$ phase near the joint interface and mixed structure of $Ti_3SiC_2$ and $TiC_x$ at the center of the joint layer. The joint layer contained micro-cracks as a pre-existing defect.

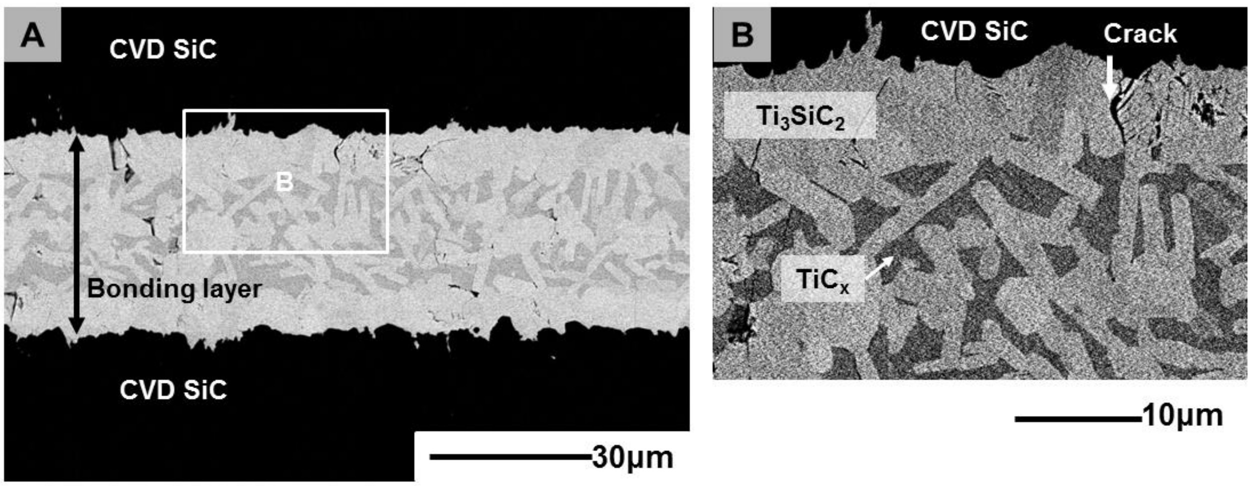


**Figure 1. Cross-sectional backscattered electron images of the Ti foil joint. Image B were taken approximately from the location indicated by rectangles in the image A.**

### 2.2.2 Molybdenum diffusion bonding

Pure molybdenum foil (25 µm thick, 99.95% pure, Alfa-Aesar, Ward Hill, MA) was used for Mo diffusion bonding. The Mo foil joints were fabricated at ORNL. The joining of SiC/metal/SiC sandwiches was accomplished by hot-pressing at 1500 °C, for 1 h, in flowing Ar-4% $H_2$ atmosphere, under a uniaxial pressure of 20 MPa. Estimated partial pressure of oxygen impurity in the furnace was ~0.02 Pa. During the hot-pressing, the presence of both hydrogen and titanium powder facilitated effective oxygen gettering. The processing condition is optimized based on the obtained microstructure and the shear strength [4].

Mo foil-joined SiC had a layered structure of $Mo_{4.8}Si_3C_{0.6}$ near the joint interface and $Mo_2C$ phases at the center of the joint layer as shown in Figure 2. The joint contained cracks roughly perpendicular to the joint boundary in the as-processed condition. The joint thickness was ~35 µm.

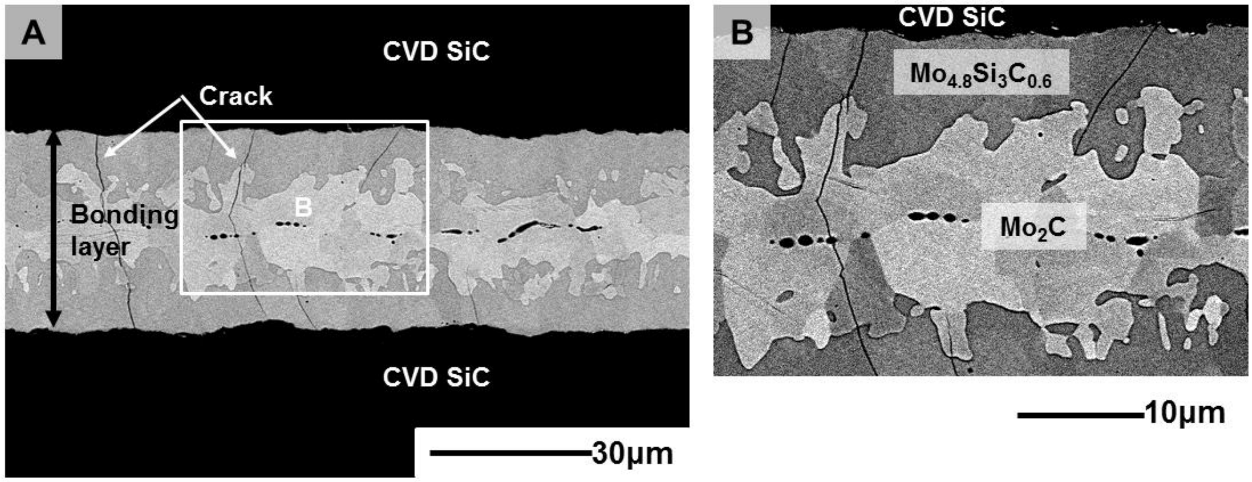


**Figure 2.** Cross-sectional backscattered electron images of the Mo foil joint (A and B). Image B were taken approximately from the location indicated by rectangles in the image A.

### 2.2.3 TEP method using SiC-based slurry and green tape

Two types of TEP joining were prepared in this work: the joining using mixed powder slurry (TEPs) and the joining with a commercial green tape (TEPt). Both joints were fabricated at Kyoto University.

To make the slurry for the TEPs joining, SiC nano-phase powder (average diameters ~30 nm), and $Al_2O_3$ powder, $Y_2O_3$ powder were dispersed in ethanol. The total amount of oxide additives was 6 wt%. For the fabrication of TEPs joint, the slurry was sandwiched by CVD SiC plates, and then dried at ~80 °C. After that, the TEPs joint was formed by hot-pressing at 1850 °C, for 1 h, in an Ar atmosphere, under a pressure of 10 MPa.

The feedstock of the green tape for the TEPt joint was same as that of the TEPs slurry except for the additional use of organic binder. The green tape was provided by in Gunze ltd. in Japan. The joining of SiC/green tape/SiC sandwiches was accomplished by hot-pressing. The hot-pressing conditions were same as those for the TEPs joint.

Cross-sectional backscattered electron image of the TEPs joint was shown in Figure 3. The joint thickness was ~80 μm. The joint layer appeared to be highly dense. In addition, the secondary phases attributed to the oxide additives were well dispersed, and up to ~5 μm-sized segregation of Y-Al oxide phase was observed. The microstructure of the TEPt joint was clearly different from the TEPs joint as shown in Figure 4. The TEPt joint was partially deboned due to the presence of large (~50 to ~100 μm) pores. In addition, lineal segregation of the secondary phases was observed in the bonding layer, which was not present in the TEPs joint. The joint thickness of the TEPt joint was ~150 μm.

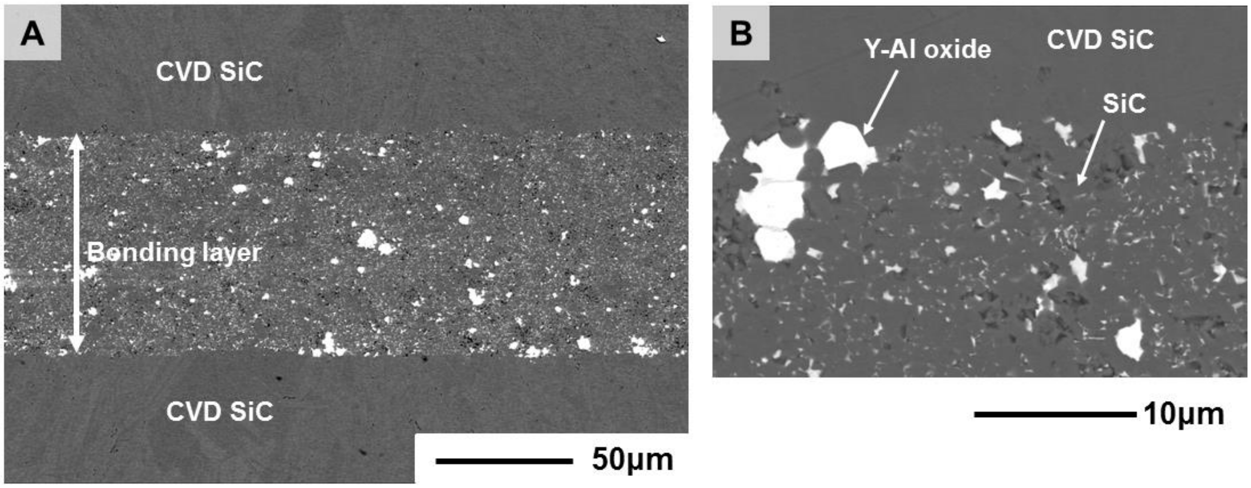


**Figure 3.** Cross-sectional backscattered electron images of the TEPs joint (A and B). Micrograph B is magnified image of the joint interface.

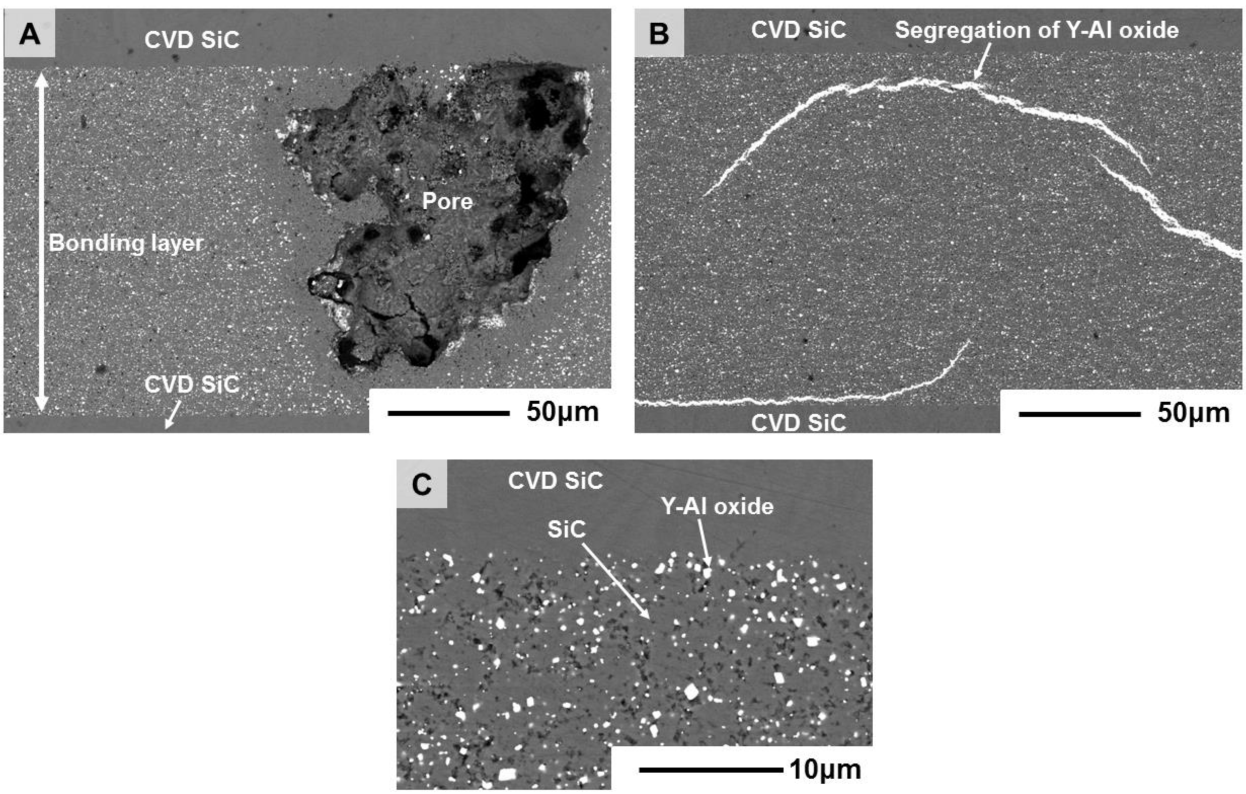


**Figure 4.** Cross-sectional backscattered electron images of the TEPt joint (A –C). Micrograph C is magnified image of the joint interface.

### 2.2.4 Reaction-formed Ti-Si-C MAX-phase bonding

For MAX phase bonding, a set of joining agent materials were purchased from Hyper-Therm High Temperature Composites, Inc. (currently Rolls-Royce High Temperature Composites, Inc., Huntington Beach, CA). Ti-Si-C phase-based joints of CVD SiC were produced at ORNL based on a pressure-less slurry process per the Hyper-Therm formula. Details of the raw materials and the process conditions are proprietary.

Cross-sectional backscattered electron image of the joint layer was shown in Figure 5. The joint layer appeared to be dense, and the joint thickness was about 150 µm. The bonded zone consisted of SiC grains and Ti-Si-C phase. The Ti-Si-C phases were expected to be mainly $Ti_3SiC_2$, and the small amount of Ti-C and Si rich Ti-Si-C phases [5]. The dominant processing defect in the joint layer was crack roughly perpendicular to the joint boundary.

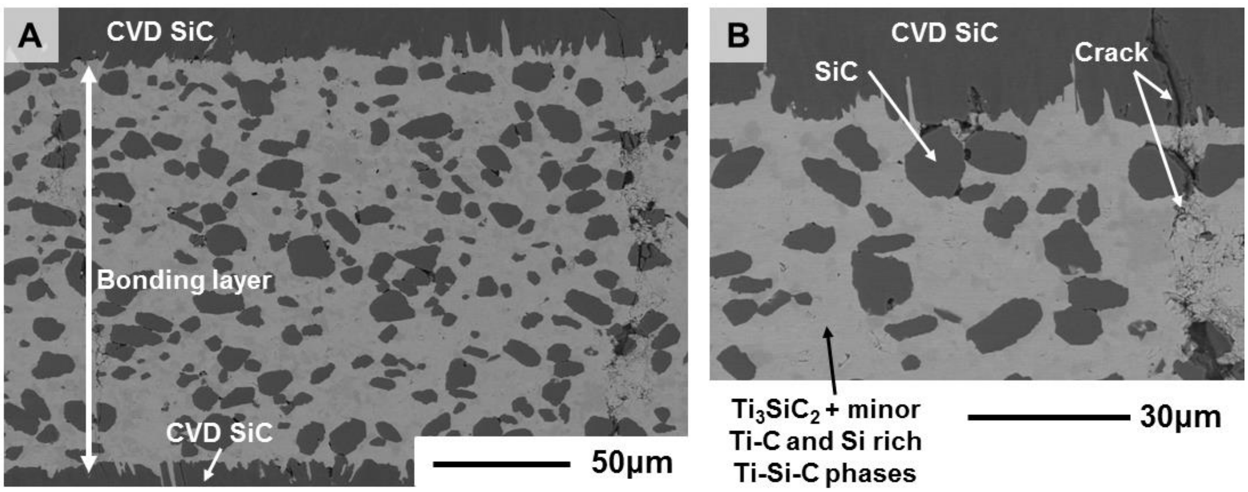


**Figure 5.** Cross-sectional backscattered electron images of the Ti-Si-C MAX phase joint (A and B). Micrograph B is magnified image of the joint interface.

### 2.2.5 Al-Si-C-O brazing

The brazed CVD SiC joint was prepared using Al-Si-C-O system by Ceramatec, Inc. in Utah. The starting materials of the brazing filler metal and the processing conditions are proprietary. The joint thickness was very thin (~3 µm) as shown in Figure 6. The brazed area consisted of complex phases; Al-C-O (phase 1 in Figure 6 (A)), Al-Si-C-O (phase 2 in Figure 6 (A)), Al-O, and Si rich phases were detected by SEM-EDS analysis. In addition, a few micron-sized pores also existed in the bonding layer.

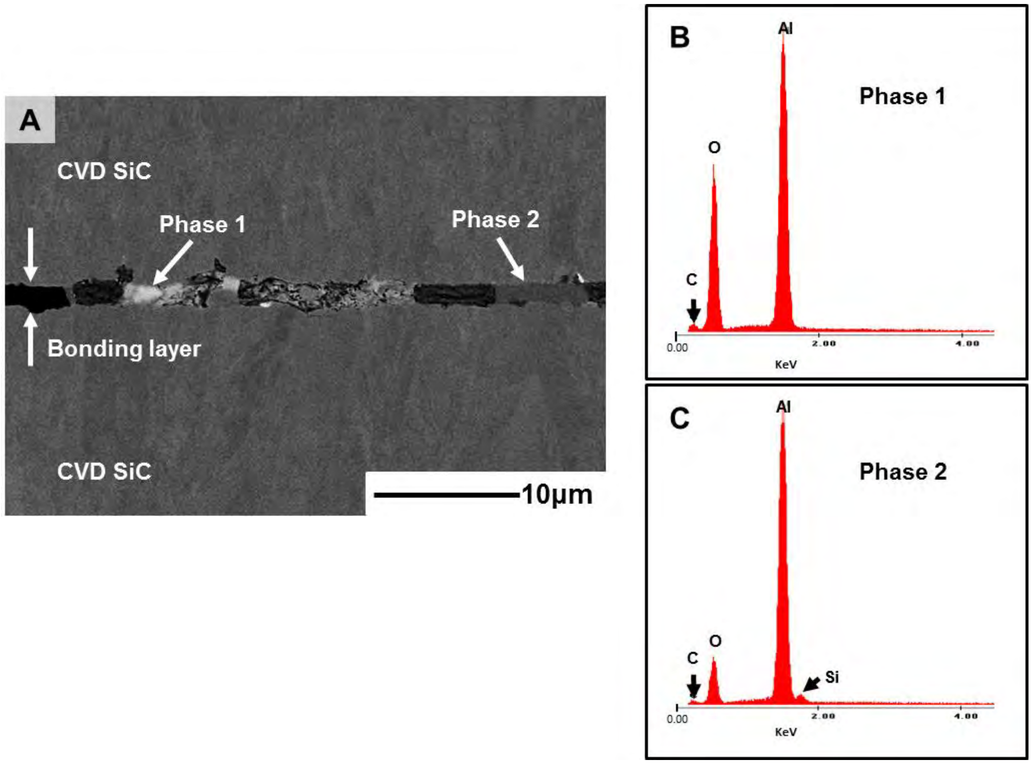


**Figure 6.** Cross-sectional backscattered electron image of the Al-Si-C-O braze-based joint (A). EDS spectrums of phase 1 and 2 indicated in image A are shown in image B and C, respectively.

### 2.2.6 Hybrid preceramic polymer/CVD joining

CVD SiC joint formed by a hybrid preceramic polymer/CVI process was provided by General Atomics in California. This joining method can provide SiC bonding layer between CVD SiC substrates. In addition, side surface of the bonded material was over-coated by SiC layer. The starting materials and the processing conditions are proprietary. Three types of the joints formed in different processing conditions were used for the irradiation experiment, and they are referred to as GA3, GA6, and GA7 in this report. Crass-sectional secondary electron images of these joints are shown in Figure 7. These joints exhibited similar microstructure among them. The bonding later between CVD SiC substrates was a 5 mm-thick layer and was partially deboned. The over-coating layer at the side surface of the joint consisted of ~20 μm-thick dense SiC layer at the very surface and porous SiC between the dense SiC layer and SiC substrate. Thickness of the overcoat varied from 100 to 300 μm.

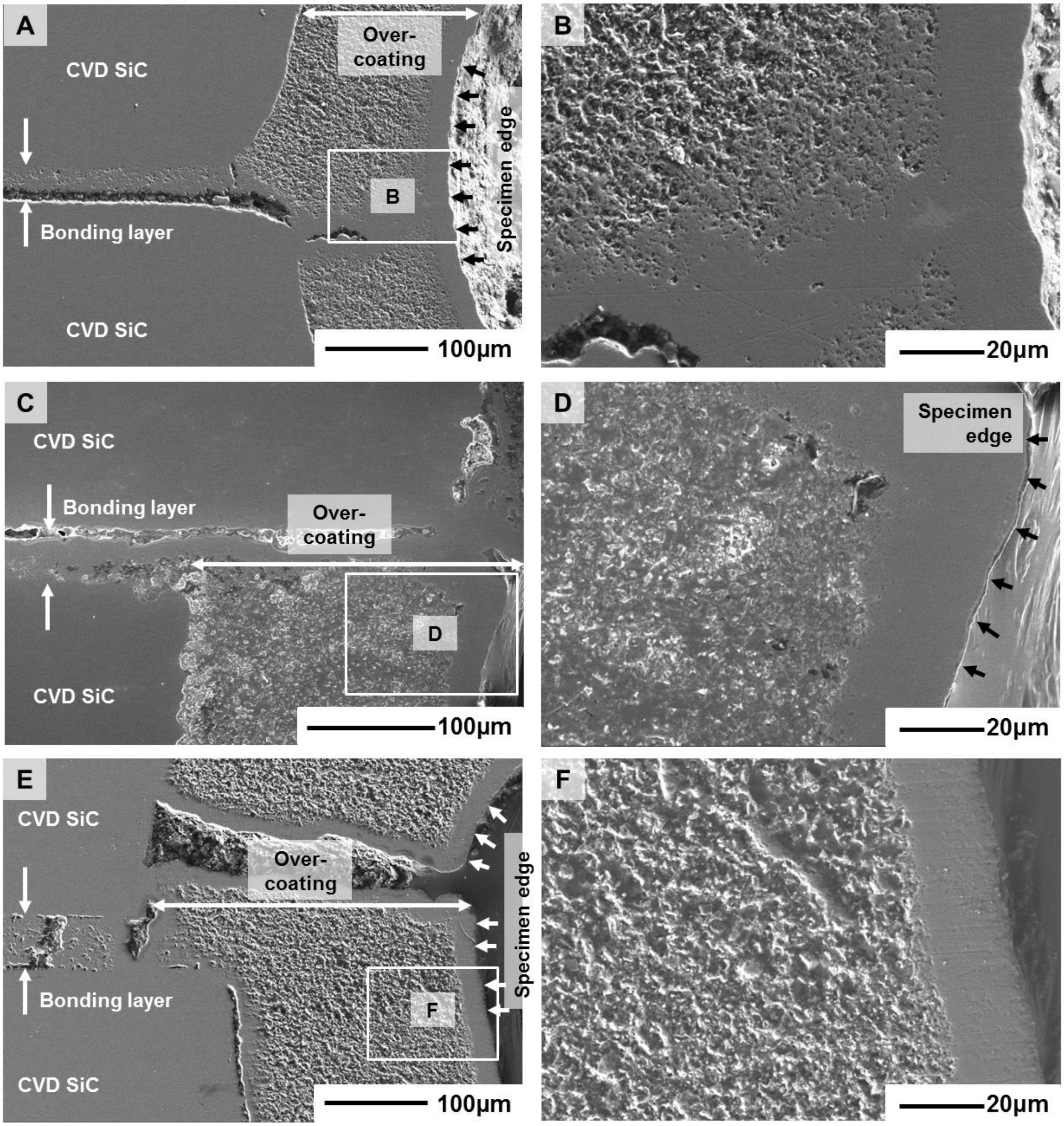


**Figure 7**. Crass-sectional secondary electron images of three types of hybrid preceramic polymer/CVI joints (A and B: GA3, C and D: GA6, E and F: GA7). Micrographs B, D, and F were taken approximately from locations shown by rectangles in micrographs A, C, and E, respectively. Specimen edge is arrowed in image A, D, and E.

## 2.3 MECHANICAL PROPERTIES

**Shear strength of the joint test specimens was evaluated by the torsional shear testing of hourglass-type specimens that had specifically been designed and established for neutron irradiation studies [6-8]. The specimens used are shown in**

Figure 8.

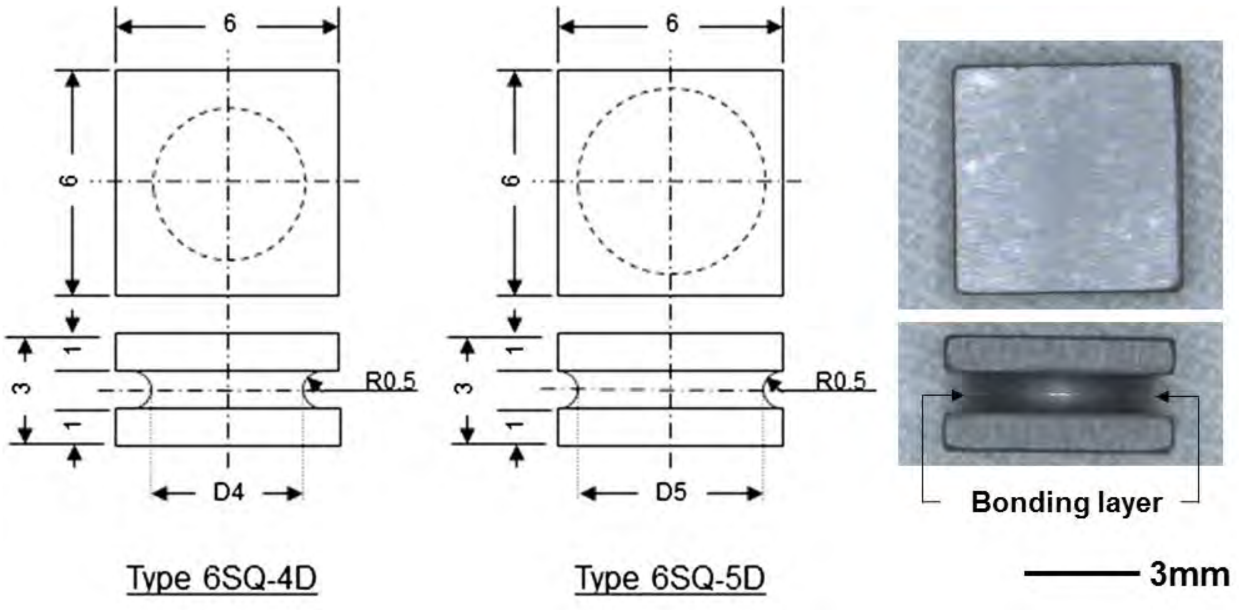


**Figure 8.** Drawing of 6SQ-4D and -5D torsion specimens, and appearance of machined Ti foil bonded SiC. Unite of drawing is mm.

Results of pre-irradiation torsion tests on various SiC joints are summarized in Figure 9. The fracture appearance is also indicated in the figure. Three to ten specimens were tested for each joint. Note that the round surface of torsion specimens for hybrid preceramic polymer/CVI joining were over-coated as shown in Figure 7. Ti foil, Mo foil, TEPt, MAX phase, and brazed joints mostly exhibited shear strength of 100 to 150 MPa. All specimens for these joints failed at the SiC substrate as shown in Figure 10 (A). It is difficult to identify the location of the crack initiation for these joints, because the neck part of the specimen got shattered into pieces after the test. TEPs joints also exhibited the failure at the SiC substrate. On the other hand, the shear strength was extremely high (>300 MPa for all tested specimens). Relatively weak shear strengths (mostly less than 100 MPa) were obtained from three types of hybrid preceramic polymer/CVI joined specimens. These specimens failed completely or partially at the joint plane as shown in Figure 10 (B and C). Note that the torsional shear strength evaluated in this work may be affected by not only the bonding strength but also residual stress, surface condition, and differential elastic modulus between bonding layer and SiC substrate.

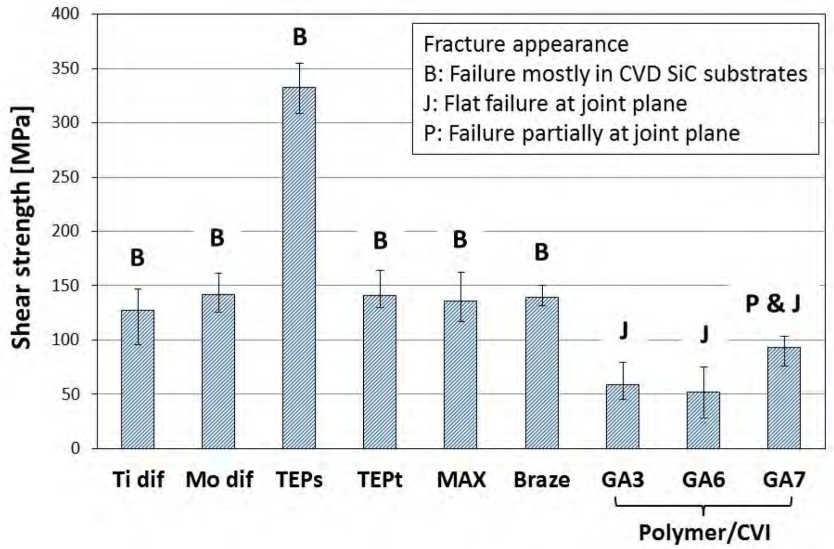


**Figure 9.** Shear strength of various SiC joints investigated by torsional test before irradiation. The highest and lowest error bars indicate maximum and minimum strength, respectively. Fracture appearance is also indicated. Refer to **Table 1** for aliases used for joint identification.

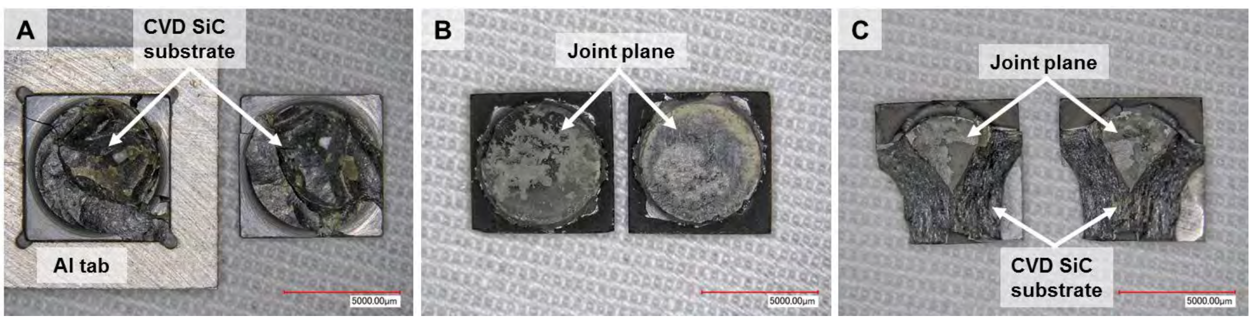


**Figure 10. Typical fracture appearance of torsion tested specimens: failure in CVD SiC substrate (A), failure at joint plane (B), and failure partially at joint plane (C).**

## 3. IRRADIATION MATRIX

Three rabbit capsules are being irradiated in target rod rabbit holders position (position TRRH7) in HFIR. The target temperature and fluence are 300 °C and $8 \times 10^{25}$ n/m$^2$ (E > 0.1 MeV), respectively. That fluence corresponds with dose of 8 dpa-SiC, assuming an equivalence of 1 x $10^{25}$ n/m$^2$ (E > 0.1 MeV) with 1 dpa in SiC. Each rabbit contains 16 hourglass-shaped specimens mainly for torsional shear test. The bonding layer located at the center of the specimen in 3 mm thickness direction as shown in Figure 8. The specimen types 6SQ-5D and -4D in Figure 8 were chosen for this study since our previous study demonstrated that those geometries are appropriate for the torsional test [6]. That means that 6SQ-5D and -4D specimens appeared to fail not at square grip region but at around bonded zone. The detail of the test matrix is shown in Table 2.

**Table 2. Test matrix of neutron irradiation experiment**

| Rabbit ID | Material Type | Specimen ID | Specimen Type | Diameter [mm] | Length [mm] | Width [mm] | Thickness [mm] |
|---|---|---|---|---|---|---|---|
| SCJ2-01 | Ti dif | T2 | 6SQ-5D | 5.02 | 5.98 | 5.98 | 2.97 |
| | | T6 | 6SQ-5D | 5.01 | 5.98 | 5.98 | 2.98 |
| | | T11 | 6SQ-5D | 5.08 | 5.98 | 5.98 | 2.97 |
| | | T15 | 6SQ-5D | 5.05 | 5.98 | 5.98 | 2.97 |
| | Mo dif | R6 | 6SQ-5D | 4.90 | 5.98 | 5.98 | 3.02 |
| | | R10 | 6SQ-5D | 4.96 | 5.98 | 5.98 | 3.02 |
| | | R12 | 6SQ-5D | 4.99 | 5.97 | 5.98 | 3.02 |
| | | R13 | 6SQ-5D | 4.99 | 5.97 | 5.98 | 3.02 |
| | MAX | M1 | 6SQ-5D | 5.00 | 5.95 | 5.92 | 3.00 |
| | | M2 | 6SQ-5D | 4.97 | 5.89 | 5.92 | 3.01 |
| | | M6 | 6SQ-5D | 4.98 | 5.96 | 5.95 | 3.01 |
| | | M7 | 6SQ-5D | 4.97 | 5.89 | 5.94 | 3.01 |
| | Braze | A1 | 6SQ-5D | 5.00 | 5.98 | 5.98 | 3.00 |
| | | A2 | 6SQ-5D | 4.99 | 5.98 | 5.99 | 2.99 |
| | | A3 | 6SQ-5D | 5.00 | 5.98 | 5.98 | 2.99 |
| | | A5 | 6SQ-5D | 5.02 | 5.98 | 5.98 | 2.99 |
| SCJ2-02 | TEPs | K4 | 6SQ-4D | 3.91 | 5.99 | 6.00 | 2.97 |
| | | K8 | 6SQ-4D | 3.96 | 6.00 | 6.00 | 2.97 |
| | | K13 | 6SQ-4D | 3.93 | 6.00 | 5.99 | 2.97 |
| | | K14 | 6SQ-4D | 3.90 | 6.00 | 5.99 | 2.97 |
| | | K15 | 6SQ-4D | 3.96 | 6.00 | 6.00 | 2.97 |
| | TEPt | G1 | 6SQ-4D | 3.87 | 5.99 | 6.00 | 2.97 |
| | | G2 | 6SQ-4D | 3.90 | 5.99 | 5.99 | 2.97 |
| | | G7 | 6SQ-4D | 3.89 | 5.97 | 5.99 | 2.97 |
| | | G8 | 6SQ-4D | 3.90 | 6.00 | 6.00 | 2.97 |
| | | G9 | 6SQ-4D | 3.89 | 5.99 | 5.99 | 2.97 |
| | Ti dif | T14 | 6SQ-5D | 5.02 | 5.98 | 5.98 | 2.97 |
| | Mo dif | R1 | 6SQ-5D | 5.04 | 5.98 | 5.98 | 3.02 |
| | MAX | M3 | 6SQ-5D | 4.99 | 5.97 | 5.96 | 3.01 |
| | | M4 | 6SQ-5D | 4.99 | 5.95 | 5.95 | 3.01 |
| | Braze | A6 | 6SQ-5D | 5.01 | 5.98 | 5.98 | 3.00 |
| | | A7 | 6SQ-5D | 4.97 | 5.97 | 5.98 | 3.00 |
| SCJ2-03 | Polymer/CVI (GA3) | 03 | 6SQ-5D | 4.89 | 6.00 | 5.98 | 2.94 |
| | | 06 | 6SQ-5D | 4.92 | 6.00 | 6.00 | 2.94 |
| | | 07 | 6SQ-5D | 4.93 | 5.99 | 5.99 | 2.96 |
| | | 08 | 6SQ-5D | 5.15 | 5.97 | 5.96 | 2.96 |
| | | 09 | 6SQ-5D | 5.02 | 5.99 | 5.99 | 2.95 |
| | Polymer/CVI (GA6) | 6 06 | 6SQ-5D | 5.06 | 5.97 | 5.97 | 2.87 |
| | | 6 07 | 6SQ-5D | 5.58 | 5.97 | 5.99 | 2.89 |
| | | 6 08 | 6SQ-5D | 5.15 | 5.91 | 5.93 | 2.89 |
| | | 6 09 | 6SQ-5D | 5.12 | 5.99 | 5.99 | 2.89 |
| | | 6 10 | 6SQ-5D | 5.08 | 5.94 | 5.94 | 2.90 |
| | Polymer/CVI (GA7) | 7 01 | 6SQ-5D | 4.90 | 5.95 | 5.97 | 2.89 |
| | | 7 02 | 6SQ-5D | 4.78 | 5.97 | 5.97 | 2.90 |
| | | 7 03 | 6SQ-5D | 4.95 | 5.98 | 5.97 | 2.91 |
| | | 7 04 | 6SQ-5D | 5.21 | 6.00 | 5.97 | 2.85 |
| | | 7 05 | 6SQ-5D | 5.20 | 5.97 | 5.97 | 2.91 |
| | Braze | A13 | 6SQ-5D | 4.98 | 5.98 | 5.98 | 2.99 |

## 4. PLAN OF POST-IRRADIATION EXPERIMENT

More than four samples are being irradiated for each type of joint. At least three samples will be used for torsional shear test to investigate effect of irradiation on the mechanical property. The remaining sample will be used for microstructural observation and as a possible back-up shear test specimen.

The torsion test will be conducted on hour-glass specimens in Figure 8 using TestResources 160GT-125Nm torsion system with flexible couplers and sample grips (Figure 11.). Ideally, maximum shear stress is applied at the rounded surface of bonding layer during testing, according to the finite-element stress method analysis [6]. The flexible couplers were used to keep the alignment during testing. Aluminum-alloy tabs were installed at the square grip sections to obtain uniform stress distributions there. The rotation speed was 0.15 deg/min. Nominal shear strength values ($\tau$) in this work are given by following equation,

$$\tau = 16T/\pi d^3 \quad (1)$$

where $T$ is the applied torque and $d$ is the specimen diameter of the neck. Further description of details of the test method can be found elsewhere [6]. All the torsion tests will be conducted at room temperature. The details of the fracture behavior will be investigated using optical microscope (KEYENCE, VHX-1000). The effect of irradiation on the strength will be discussed using the strength value and the fracture appearance before and after irradiation.

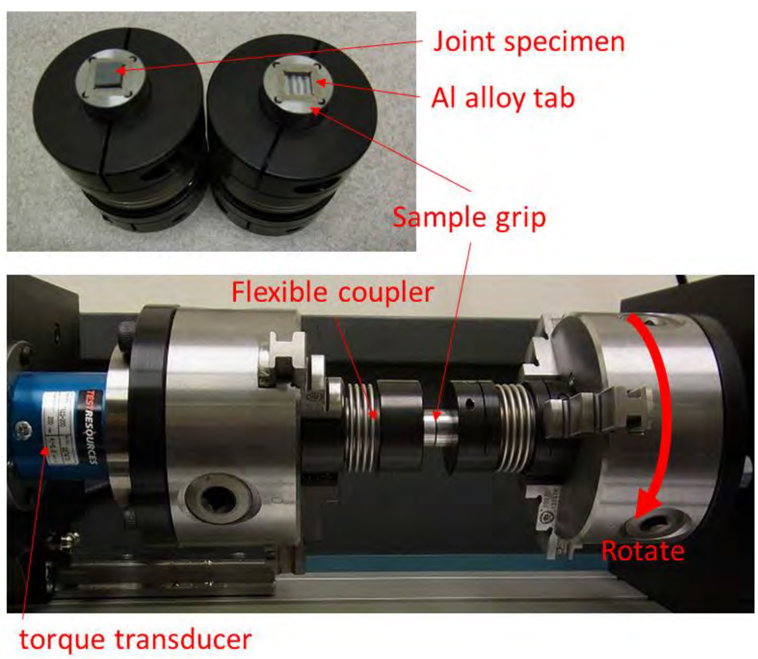


**Figure 11**. Appearance of torsional test system to evaluate shear strength of joint specimen.

Microstructural observation of the joint layer in as-irradiated samples is planned using with a Hitachi S4700 SEM. Stability of the joint phases and presence or absence of irradiation-induced cracking caused by differential swelling between the joint layer and the SiC substrate will be investigated.

XRD is also planned to identify phases in irradiated bonding layer. The sample for XRD will be torsion tested specimen which exhibits failure at the joint plane, because a certain amount of surface area is required for the XRD analysis.

An actual irradiation temperature will be determined by dimensional change of CVD SiC parts irradiated with the SiC joints upon annealing, using a dilatometer. As the SiC parts were designed to be in direct contact with the joint specimens during irradiation, this measurement can represent an accurate sample temperature during irradiation.

## 5. SCHEDULE

It will take 6 HFIR cycles to achieve the target fluence of 8 dpa in the positions where the rabbit capsules are being irradiated. The irradiation started from the beginning of Cycle 453 on 5/6/2014 and is anticipated to end at the end of Cycle 458 (estimated date 2/6/2015 according to the current planning schedule of HFIR operation). The current HFIR operating schedule is shown in Table 4. Following the irradiation, the rabbit capsules will be kept at the storage area for at least a month for cooling. After that, the capsules will be disassembled in 3025E hot-cell facility at ORNL to take out the joint specimens. The specimens will be tested at Low Activation Materials Development and Analysis (LAMDA) laboratory at ORNL when the activity of the samples is low enough to handle.

**Table 3. Irradiation schedule of rabbit capsules.**

| Capsule | Rabbit Position | Target Temperature | Target Fluence* | Estimated Fluence* at EOC458 | Estimated Date EOC458 |
|---|---|---|---|---|---|
| SCJ2-01 | C1-7 | 300°C | 8 | 8.9 | 2/06/2015 |
| SCJ2-02 | F7-7 | 300°C | 8 | 8.9 | 2/06/2015 |
| SCJ2-03 | D2-7 | 300°C | 8 | 8.9 | 2/06/2015 |

*x$10^{25}$ n/$m^2$ (E > 0.1 MeV); EOC = end of cycle

**Table 4. Operating schedule of HFIR. EOC indicates end-of-cycle for refueling outage.**

| Cycle | Start | Finish | Duration |
|---|---|---|---|
| 452 | Tue 2/25/14 | Fri 3/21/14 | 24 days |
| 452 EOC | Fri 3/21/14 | Tue 5/6/14 | 46 days |
| 453 | Tue 5/6/14 | Fri 5/30/14 | 24 days |
| 453 EOC | Fri 5/30/14 | Tue 6/17/14 | 18 days |
| 454 | Tue 6/17/14 | Fri 7/11/14 | 24 days |
| 454 EOC | Fri 7/11/14 | Tue 7/29/14 | 18 days |
| 455 | Tue 7/29/14 | Fri 8/22/14 | 24 days |
| 455 EOC | Fri 8/22/14 | Tue 10/7/14 | 46 days |
| 456 | Tue 10/7/14 | Fri 10/31/14 | 24 days |
| 456 EOC | Fri 10/31/14 | Tue 11/18/14 | 18 days |
| 457 | Tue 11/18/14 | Fri 12/12/14 | 24 days |
| 457 EOC | Fri 12/12/14 | Tue 1/13/15 | 32 days |
| 458 | Tue 1/13/15 | Fri 2/6/15 | 24 days |
| 458 EOC | Fri 2/6/15 | Tue 2/24/15 | 18 days |
| 459 | Tue 2/24/15 | Fri 3/20/15 | 24 days |
| 459 EOC | Fri 3/20/15 | Tue 6/9/15 | 81 days |
| 460 | Tue 6/9/15 | Fri 7/3/15 | 24 days |
| 460 EOC | Fri 7/3/15 | Tue 7/21/15 | 18 days |
| 461 | Tue 7/21/15 | Fri 8/14/15 | 24 days |
| 461 EOC | Fri 8/14/15 | Tue 10/6/15 | 53 days |

Start irradiation

6 cycles
Fluence: ~8dpa

End irradiation
(Plan)

According to the current HFIR schedule and assuming availability of resources for capsule transfer, disassembly, and post-irradiation examination, it is anticipated that the evaluation of irradiated test specimens starts around May 2015.

## 6. REFERENCES

[1] Y. Katoh, K.A. Terrani, L.L. Snead, ORNL/TM-2014/210, Revison 1, Systematic Technology Evaluation Program for SiC/SiC Compositebased Accident-Tolerant LWR Fuel Cladding and Core Structures, in, 2014.
[2] S. Bragg-Sitton, D. Hurley, M. Khafizov, B. Merrill, R. Schley, K. McHugh, I. van Rooyen, Y. Katoh, C. Shih, Silicon Carbide Gap Analysis and Feasibility Study, INL/EXT-13-29728, in, Idaho National Laboratory, Idaho Falls, 2013.
[3] Y. Katoh, J. Kiggans, C. Shih, T. Koyanagi, J.L. McDuffee, L.L. Snead, ORNL/TM-2013/273, Status of Silicon Carbide Joining and Irradiation Studies, in, 2013.
[4] T. Koyanagi, J. Kiggans, C. Shih, Y. Katoh, Processing and Characterization of Diffusion-Bonded Silicon Carbide Joints using Molybdenum and Titanium Interlayers, Ceramic Engineering and Science Proceedings, (Accepted for publication).
[5] T. Koyanagi, J. Kiggans, C. Shih, Y. Katoh, Process Development and Optimization for Silicon Carbide Joining and Irradiation Studies-III, Fusion Reactor Materials, DOE/ER-0313/55, (2013) 11-22.
[6] H.C. Jung, T. Hinoki, Y. Katoh, A. Kohyama, Development of a shear strength test method for NITE-SiC joining material, Journal of Nuclear Materials, 417 (2011) 383-386.
[7] Y. Katoh, L.L. Snead, T. Cheng, C. Shih, W.D. Lewis, T. Koyanagi, T. Hinoki, C.H. Henagar, M. Ferraris, Radiation-Tolerant Joining Technologies for Silicon Carbide Ceramics and Composites, Journal of Nuclear Materials, 448 (2014) 497-511.
[8] M. Ferraris, M. Salvo, V. Casalegno, A. Ventrella, M. Avalle, Torsion Tests on AV119 Epoxy – Joined SiC, International Journal of Applied Ceramic Technology, (2013) in press.

# APPENDIX A. SPECIMEN DETAILS

## APPENDIX A. SPECIMEN DETAILS

Drawings of the Type 6SQ-5D and Type 6SQ-4D torsional shear test specimens are given here.

Miniature Joint Specimen for Torsional Shear Test: Type 6SQ-5D (6x6x3 mm)

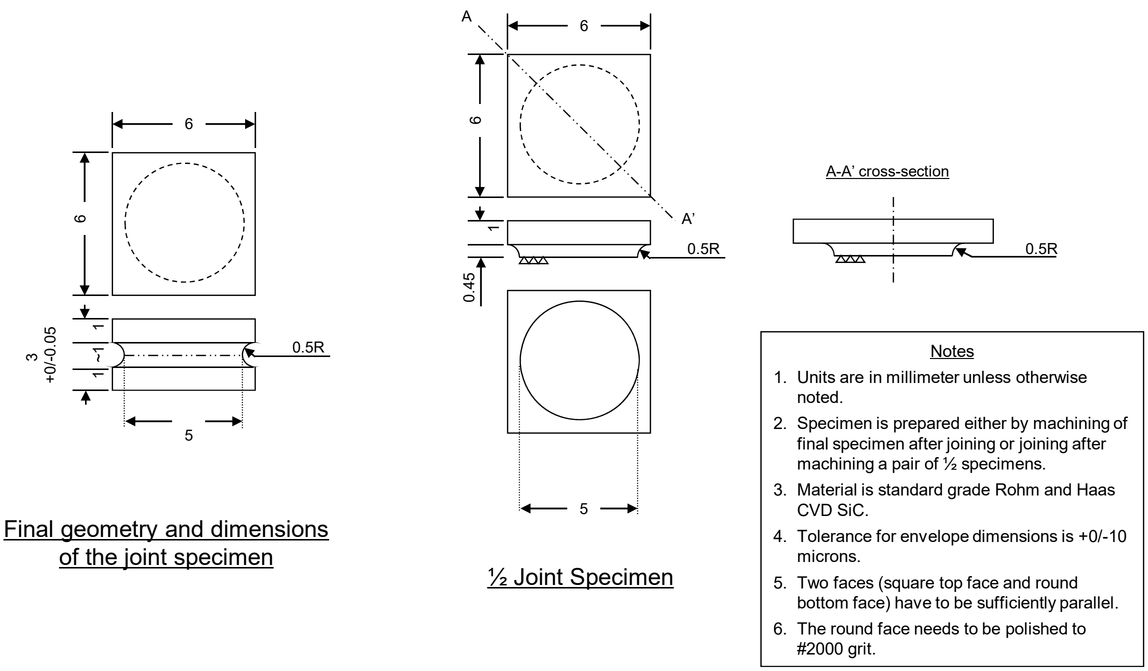


Printed 1/4/2008 3:29 PM Yutai Katoh (576-5996, A-148/4500S, katohy@ornl.gov)

## Miniature Joint Specimen for Torsional Shear Test: Type 6SQ-4D (6x6x3 mm)

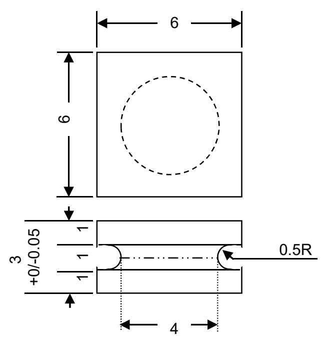


Final geometry and dimensions of the joint specimen

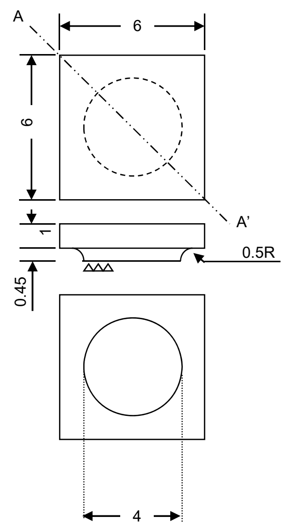


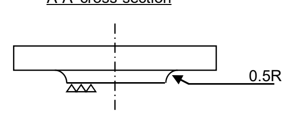


½ Joint Specimen

Notes

1. Units are in millimeter unless otherwise noted.
2. Specimen is prepared either by machining of final specimen after joining or joining after machining a pair of ½ specimens.
3. Material is standard grade Rohm and Haas CVD SiC.
4. Tolerance for envelope dimensions is +0/-10 microns.
5. Two faces (square top face and round bottom face) have to be sufficiently parallel.
6. The round face needs to be polished to #2000 grit.

Printed 1/4/2008 3:29 PM

Yutai Katoh (576-5996, A-148/4500S, katohy@ornl.gov)

# APPENDIX B.  CAPSULE DRAWINGS

## APPENDIX B. CAPSULE DRAWINGS

Conceptual and engineering design drawings of the rabbit capsules for irradiation of the torsional shear test specimens are given in this section.

### SiC Torsional Joint Capsule (Rev. 100316)

**List of internal parts (= inside sleeve) and specimens**

| Part # | Name | Material | Qty / Capsule |
|---|---|---|---|
| 1 | Thermometry Bar | CVD SiC HR grade | 2 |
| N/A | Specimen (Type 6SQ-5D) | SiC (CVD or composite) | 16 |
| ~~N/A~~ | ~~Specimen (Coupon)~~ | ~~SiC (CVD or composite)~~ | ~~8~~ |

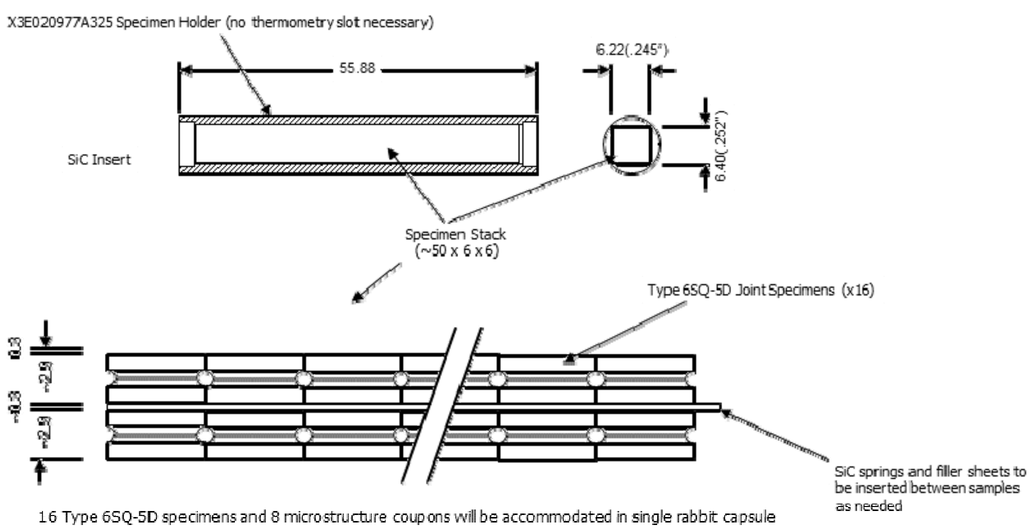


Printed 1/4/2006 3:29 PM

Yutai Katoh (576-3986, A-148/4500S, katohy@ornl.gov)

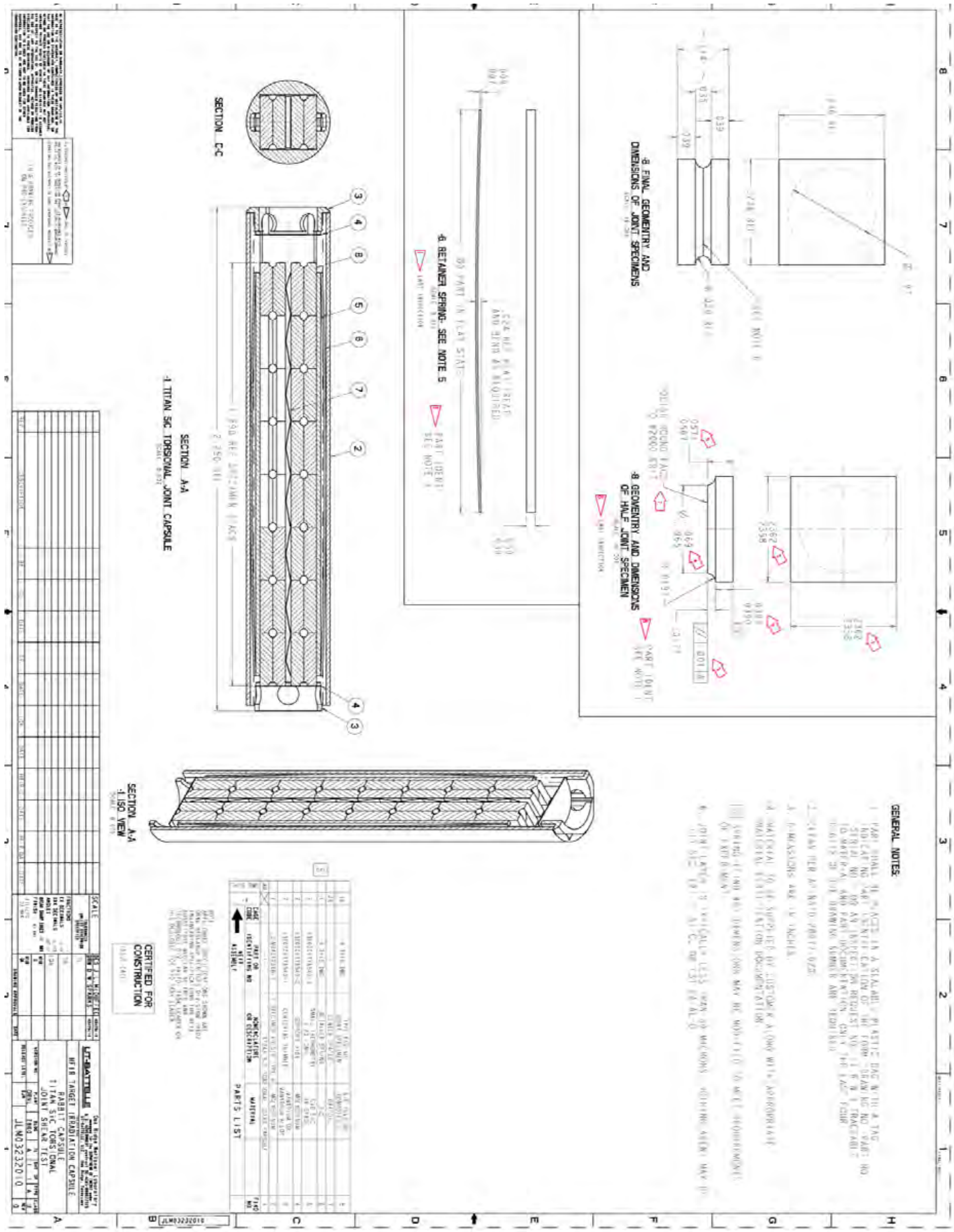
GENERAL NOTES:
SECTION C-C
SECTION A-A
-1 TITAN SiC TORSIONAL JOINT CAPSULE
-6 RETAINER SPRING- SEE NOTE 5
-8 FINAL GEOMETRY AND DIMENSIONS OF JOINT SPECIMENS
-8 GEOMETRY AND DIMENSIONS OF HALF JOINT SPECIMEN
SECTION A-A
-1 ISO VIEW
PARTS LIST
CERTIFIED FOR CONSTRUCTION
UT-BATTELLE
JLM03232010

# APPENDIX C.  THERMAL ANALYSIS RESULT

## APPENDIX C. THERMAL ANALYSIS RESULT

Result of the finite element thermal analysis of the irradiation capsule is provided in this section.

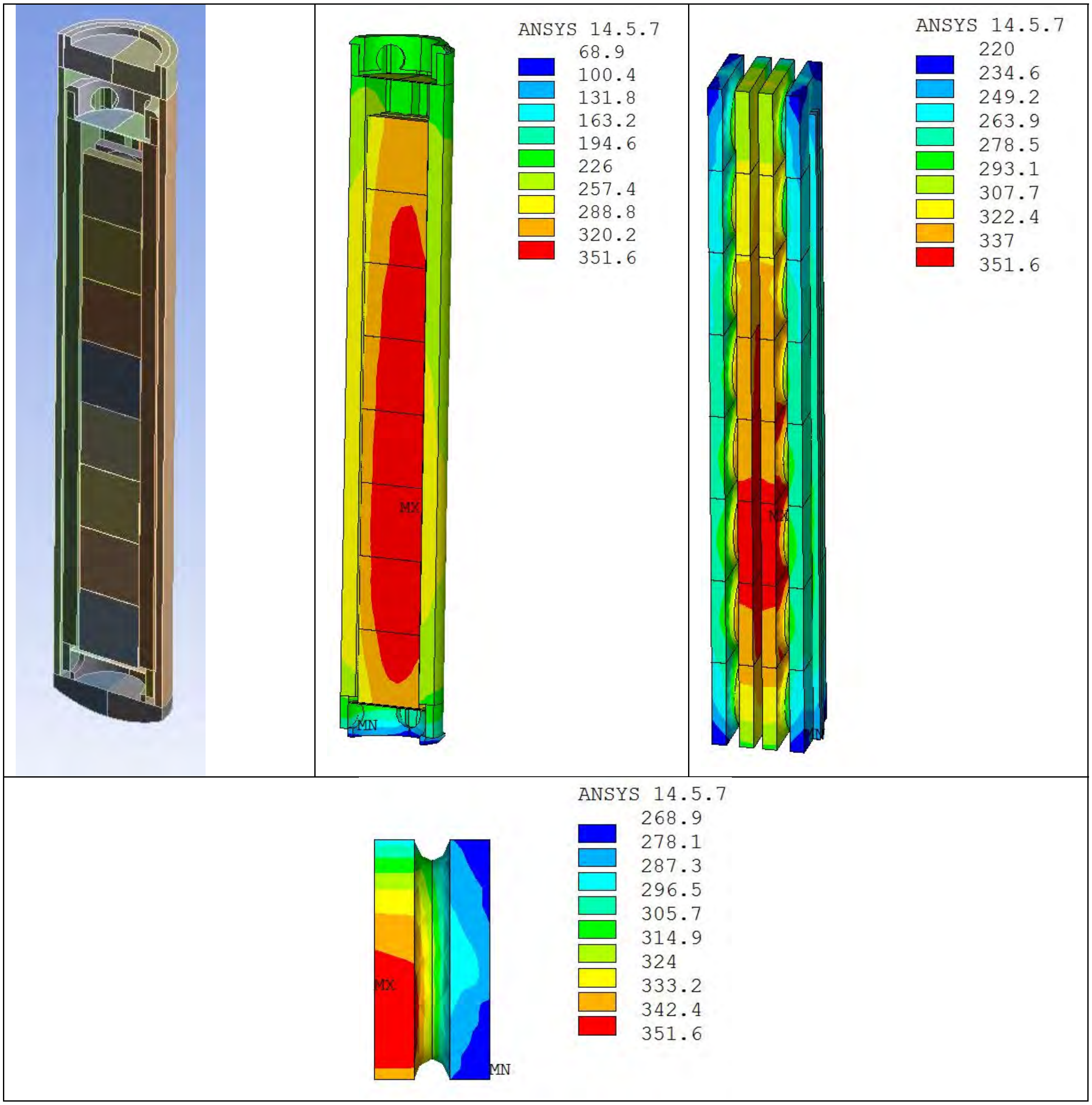


Half-cut three-dimensional model developed for thermal analysis of the SiC torsional joint rabbits (top left), temperature distribution at inside surface of specimens stack (top center), temperature distribution of the entire specimens stack (top right), and temperature distribution within one of the hot specimens (bottom). Despite the relatively large temperature distribution within the specimens stack, the joint planes are maintained in a temperature range 290 – 320 °C for all specimens.

************************************************************************
TEMPERATURE DESIGN SOLUTION FOR SiC JOINT-JOINT RABBITS
************************************************************************

DESCRIPTION

* 300.°C target temperature
* Helium fill gas
* 15.84 cm bottom location

BOUNDARY CONDITIONS

Heat transfer coefficient = 47700. W/m²•°C
Bulk coolant temperature = 53.6 °C

HEAT GENERATION

| Part | Material | Heat Gen. @Midplane (W/kg) | Heat Load @Midplane (W) | Heat Load @Location (W) |
|---|---|---|---|---|
| 1) Specimen 1D | SiC(Irr) | 31700. | 9.3 | 6.8 |
| 2) Specimen 1C | SiC(Irr) | 31700. | 9.3 | 6.8 |
| 3) Specimen 2D | SiC(Irr) | 31700. | 9.3 | 6.7 |
| 4) Specimen 2C | SiC(Irr) | 31700. | 9.3 | 6.7 |
| 5) Specimen 3D | SiC(Irr) | 31700. | 9.3 | 6.5 |
| 6) Specimen 3C | SiC(Irr) | 31700. | 9.3 | 6.5 |
| 7) Specimen 4D | SiC(Irr) | 31700. | 9.3 | 6.3 |
| 8) Specimen 4C | SiC(Irr) | 31700. | 9.3 | 6.3 |
| 9) Specimen 5D | SiC(Irr) | 31700. | 9.3 | 6.2 |
| 10) Specimen 5C | SiC(Irr) | 31700. | 9.3 | 6.2 |
| 11) Specimen 6D | SiC(Irr) | 31700. | 9.3 | 6.0 |
| 12) Specimen 6C | SiC(Irr) | 31700. | 9.3 | 6.0 |
| 13) Specimen 7D | SiC(Irr) | 31700. | 9.3 | 5.9 |
| 14) Specimen 7C | SiC(Irr) | 31700. | 9.3 | 5.9 |
| 15) Specimen 8D | SiC(Irr) | 31700. | 9.3 | 5.7 |
| 16) Specimen 8C | SiC(Irr) | 31700. | 9.3 | 5.7 |
| 17) Housing | AL-6061 | 31300. | 57.4 | 38.5 |
| 18) Housing | AL-6061 | 31300. | 57.4 | 38.5 |
| 19) Housing upper | AL-6061 | 31300. | 2.6 | 1.5 |
| 20) Housing upper | AL-6061 | 31300. | 2.6 | 1.5 |
| 21) Housing lower | AL-6061 | 31300. | 7.6 | 5.7 |
| 23) Housing lower | AL-6061 | 31300. | 7.6 | 5.7 |
| 25) Housing end cap | AL-6061 | 31300. | 8.2 | 4.8 |
| 26) Housing end cap | AL-6061 | 31300. | 8.2 | 4.8 |
| 27) Holder | V-4Cr4Ti | 45900. | 160.1 | 107.7 |
| 29) Holder | V-4Cr4Ti | 45900. | 160.3 | 107.8 |
| 30) Holder upper | V-4Cr4Ti | 45900. | 6.0 | 3.6 |
| 31) Holder upper | V-4Cr4Ti | 45900. | 6.0 | 3.6 |
| 33) Holder lower | V-4Cr4Ti | 45900. | 6.3 | 4.7 |
| 34) Holder lower | V-4Cr4Ti | 45900. | 6.3 | 4.7 |
| 36) Cent.Thimble (lower) | Ti-6Al4V | 35200. | 2.2 | 1.7 |
| 37) Cent.Thimble (lower) | Ti-6Al4V | 35200. | 2.2 | 1.7 |
| 38) Disk lower | Ti-6Al4V | 35200. | 0.3 | 0.2 |
| 39) Disk lower | Ti-6Al4V | 35200. | 0.3 | 0.2 |
| 40) Thermometry | SiC(Irr) | 31700. | 2.2 | 1.5 |
| 41) Thermometry | SiC(Irr) | 31700. | 2.2 | 1.5 |
| 42) Spring thermometry | SiC(Irr) | 31700. | 0.9 | 0.6 |
| 43) Spring thermometry | SiC(Irr) | 31700. | 0.9 | 0.6 |
| 44) Disk upper | Ti-6Al4V | 35200. | 0.3 | 0.2 |
| 45) Disk upper | Ti-6Al4V | 35200. | 0.3 | 0.2 |

| | | | | | |
|---|---|---|---|---|---|
| 46) Cent.Thimble (upper) | Ti-6Al4V | 35200. | 2.2 | 1.3 |
| 47) Cent.Thimble (upper) | Ti-6Al4V | 35200. | 2.2 | 1.3 |
| | | | 660.7 | 444.1 |

CAPSULE TEMPERATURE SUMMARY

| Name | Material | Tavg | Tmin | Tmax | T.025 | T.975 |
|---|---|---|---|---|---|---|
| 1) Specimen 1D | SiC(Irr) | 261. | 220. | 309. | 231. | 282. |
| 2) Specimen 1C | SiC(Irr) | 311. | 242. | 338. | 269. | 333. |
| 3) Specimen 2D | SiC(Irr) | 284. | 258. | 322. | 269. | 299. |
| 4) Specimen 2C | SiC(Irr) | 333. | 279. | 349. | 297. | 348. |
| 5) Specimen 3D | SiC(Irr) | 287. | 269. | 325. | 276. | 301. |
| 6) Specimen 3C | SiC(Irr) | 337. | 291. | 352. | 301. | 350. |
| 7) Specimen 4D | SiC(Irr) | 285. | 265. | 321. | 274. | 299. |
| 8) Specimen 4C | SiC(Irr) | 334. | 287. | 349. | 299. | 348. |
| 9) Specimen 5D | SiC(Irr) | 281. | 261. | 318. | 269. | 295. |
| 10) Specimen 5C | SiC(Irr) | 329. | 282. | 344. | 294. | 342. |
| 11) Specimen 6D | SiC(Irr) | 276. | 255. | 311. | 264. | 290. |
| 12) Specimen 6C | SiC(Irr) | 322. | 276. | 338. | 288. | 335. |
| 13) Specimen 7D | SiC(Irr) | 268. | 245. | 304. | 255. | 282. |
| 14) Specimen 7C | SiC(Irr) | 313. | 265. | 330. | 280. | 327. |
| 15) Specimen 8D | SiC(Irr) | 254. | 221. | 292. | 234. | 270. |
| 16) Specimen 8C | SiC(Irr) | 300. | 241. | 318. | 265. | 315. |
| 17) Housing | AL-6061 | 58. | 56. | 62. | 56. | 60. |
| 18) Housing | AL-6061 | 58. | 55. | 62. | 56. | 59. |
| 19) Housing upper | AL-6061 | 56. | 56. | 57. | 56. | 56. |
| 20) Housing upper | AL-6061 | 56. | 55. | 56. | 56. | 56. |
| 21) Housing lower | AL-6061 | 65. | 60. | 67. | 61. | 67. |
| 23) Housing lower | AL-6061 | 65. | 60. | 68. | 61. | 67. |
| 25) Housing end cap | AL-6061 | 70. | 68. | 71. | 69. | 71. |
| 26) Housing end cap | AL-6061 | 71. | 70. | 72. | 70. | 71. |
| 27) Holder | V-4Cr4Ti | 262. | 196. | 289. | 218. | 285. |
| 29) Holder | V-4Cr4Ti | 250. | 196. | 276. | 214. | 269. |
| 30) Holder upper | V-4Cr4Ti | 208. | 191. | 222. | 195. | 218. |
| 31) Holder upper | V-4Cr4Ti | 205. | 191. | 215. | 195. | 212. |
| 33) Holder lower | V-4Cr4Ti | 195. | 151. | 233. | 166. | 221. |
| 34) Holder lower | V-4Cr4Ti | 192. | 156. | 221. | 167. | 214. |
| 36) Cent.Thimble (lower) | Ti-6Al4V | 147. | 69. | 228. | 89. | 209. |
| 37) Cent.Thimble (lower) | Ti-6Al4V | 146. | 73. | 227. | 90. | 208. |
| 38) Disk lower | Ti-6Al4V | 259. | 211. | 308. | 219. | 304. |
| 39) Disk lower | Ti-6Al4V | 266. | 211. | 310. | 220. | 309. |
| 40) Thermometry | SiC(Irr) | 267. | 237. | 282. | 242. | 278. |
| 41) Thermometry | SiC(Irr) | 267. | 237. | 282. | 242. | 278. |
| 42) Spring thermometry | SiC(Irr) | 257. | 221. | 270. | 232. | 268. |
| 43) Spring thermometry | SiC(Irr) | 257. | 221. | 270. | 232. | 268. |
| 44) Disk upper | Ti-6Al4V | 233. | 207. | 246. | 216. | 245. |
| 45) Disk upper | Ti-6Al4V | 230. | 206. | 246. | 214. | 244. |
| 46) Cent.Thimble (upper) | Ti-6Al4V | 211. | 163. | 219. | 199. | 218. |
| 47) Cent.Thimble (upper) | Ti-6Al4V | 209. | 163. | 214. | 198. | 214. |
| ALL SPECIMENS | SiC(Irr) | 298. | 220. | 352. | 249. | 347. |

PROPERTY SUMMARY AT THE AVERAGE PART TEMPERATURE

| | | Thermal Cond. | Thermal Exp. Coeff. | Emis |
|---|---|---|---|---|

| Name | Material | (W/m•ºC) | (µm/m•°C) | (---) |
|---|---|---|---|---|
| 1) Specimen 1D | SiC(Irr) | 6.651 | 3.14 | 0.900 |
| 2) Specimen 1C | SiC(Irr) | 6.627 | 3.30 | 0.900 |
| 3) Specimen 2D | SiC(Irr) | 6.640 | 3.22 | 0.900 |
| 4) Specimen 2C | SiC(Irr) | 6.618 | 3.36 | 0.900 |
| 5) Specimen 3D | SiC(Irr) | 6.639 | 3.23 | 0.900 |
| 6) Specimen 3C | SiC(Irr) | 6.616 | 3.37 | 0.900 |
| 7) Specimen 4D | SiC(Irr) | 6.640 | 3.22 | 0.900 |
| 8) Specimen 4C | SiC(Irr) | 6.617 | 3.36 | 0.900 |
| 9) Specimen 5D | SiC(Irr) | 6.641 | 3.21 | 0.900 |
| 10) Specimen 5C | SiC(Irr) | 6.619 | 3.35 | 0.900 |
| 11) Specimen 6D | SiC(Irr) | 6.644 | 3.19 | 0.900 |
| 12) Specimen 6C | SiC(Irr) | 6.623 | 3.33 | 0.900 |
| 13) Specimen 7D | SiC(Irr) | 6.648 | 3.16 | 0.900 |
| 14) Specimen 7C | SiC(Irr) | 6.627 | 3.31 | 0.900 |
| 15) Specimen 8D | SiC(Irr) | 6.654 | 3.12 | 0.900 |
| 16) Specimen 8C | SiC(Irr) | 6.633 | 3.27 | 0.900 |
| 17) Housing | AL-6061 | 166.480 | 24.21 | 0.050 |
| 18) Housing | AL-6061 | 166.452 | 24.21 | 0.050 |
| 19) Housing upper | AL-6061 | 166.177 | 24.21 | 0.050 |
| 20) Housing upper | AL-6061 | 166.163 | 24.21 | 0.050 |
| 21) Housing lower | AL-6061 | 167.223 | 24.21 | 0.050 |
| 23) Housing lower | AL-6061 | 167.248 | 24.21 | 0.050 |
| 25) Housing end cap | AL-6061 | 167.897 | 24.21 | 0.050 |
| 26) Housing end cap | AL-6061 | 167.949 | 24.21 | 0.050 |
| 27) Holder | V-4Cr4Ti | 32.582 | 9.71 | 0.350 |
| 29) Holder | V-4Cr4Ti | 32.449 | 9.69 | 0.350 |
| 30) Holder upper | V-4Cr4Ti | 32.029 | 9.65 | 0.350 |
| 31) Holder upper | V-4Cr4Ti | 31.998 | 9.65 | 0.350 |
| 33) Holder lower | V-4Cr4Ti | 31.910 | 9.64 | 0.350 |
| 34) Holder lower | V-4Cr4Ti | 31.886 | 9.63 | 0.350 |
| 36) Cent.Thimble (lower) | Ti-6Al4V | 9.467 | 9.65 | 0.320 |
| 37) Cent.Thimble (lower) | Ti-6Al4V | 9.452 | 9.65 | 0.320 |
| 38) Disk lower | Ti-6Al4V | 11.787 | 9.81 | 0.334 |
| 39) Disk lower | Ti-6Al4V | 11.899 | 9.82 | 0.338 |
| 40) Thermometry | SiC(Irr) | 6.648 | 3.16 | 0.900 |
| 41) Thermometry | SiC(Irr) | 6.648 | 3.16 | 0.900 |
| 42) Spring thermometry | SiC(Irr) | 6.652 | 3.13 | 0.900 |
| 43) Spring thermometry | SiC(Irr) | 6.653 | 3.13 | 0.900 |
| 44) Disk upper | Ti-6Al4V | 11.205 | 9.75 | 0.320 |
| 45) Disk upper | Ti-6Al4V | 11.143 | 9.75 | 0.320 |
| 46) Cent.Thimble (upper) | Ti-6Al4V | 10.734 | 9.70 | 0.320 |
| 47) Cent.Thimble (upper) | Ti-6Al4V | 10.680 | 9.69 | 0.320 |

---

RADIAL DIMENSIONS AND GAP SUMMARY FOR THE HOLDER-HOUSING GAP

| | Minimum | Maximum | Average |
|---|---|---|---|
| Contact status | 1.0 | 1.0 | 1.0 |
| Contact temperature (°C) | 122. | 211. | 185. |
| Target temperature (°C) | 57. | 60. | 59. |
| Gap (µm) | 174.340 | 183.622 | 177.309 |
| Contact pressure (MPa) | 0.000 | 0.000 | 0.000 |
| Conductance coefficient (W/m$^2$•°C) | 982. | 1130. | 1081. |
| Total heat flux (kW/m$^2$) | 101.65 | 249.97 | 203.15 |
| Gap conductance heat flux (kW/m$^2$) | 101.59 | 249.72 | 203.01 |
| Radiation heat flux (kW/m$^2$) | 0.06 | 0.23 | 0.17 |
| Contact conduction heat flux (kW/m$^2$) | 0.00 | 0.00 | 0.00 |

## INTERNAL DISTRIBUTION

1. L.L. Snead
2. M. Snead
3. K.A. Terrani
4. R.K. Nanstad
5. J.T. Busby
6. ORNL Office of Technical Information and Classification

## EXTERNAL DISTRIBUTION

7. S. Bragg-Sitton, Idaho National Laboratory
8. J. Carmack, Idaho National Laboratory